

Differential thermal analysis of the Al + 20% (Fe–50%B) system

J. Abenojar*, F. Velasco, M.A. Martinez

Department of Materials Science and Engineering, University Carlos III of Madrid, Av. Universidad, 30. E-28911 Leganes, Spain

Received 21 July 2005; received in revised form 21 December 2005; accepted 21 December 2005

Available online 31 January 2006

Abstract

In the present study, aluminium and mechanically alloyed (36 h) Fe/B (50 wt%) are mixed. Al + 20 (wt%) Fe/B mixture has been studied by differential thermal analysis to determine the aluminium quantity that is supposed to melt and afterwards does not solidify as it reacts with Fe/B powder. The different areas between endothermic reaction (melting peak) and exothermic reaction (solidification peak) allow in knowing the quantity of aluminium that reacts with Fe/B and the amount of intermetallic phases formed at high temperature. In order to follow the process, compacts were sintered at different temperatures (700, 800, 900, 1000 and 1200 °C), in N₂/10H₂/0.1CH₄ atmosphere. Microstructure was evaluated by image analysis and the results obtained by both techniques are compared. © 2006 Elsevier Inc. All rights reserved.

Keywords: Differential thermal analysis; Image analysis; Intermetallic; Borides

1. Introduction

Thermal analysis includes several techniques that enable to evaluate some physical and chemical properties of a sample after a temperature cycle. It is not only an analytical tool, but a powerful tool for engineering, thus its importance.

Parameters measured by means of a differential thermal analysis (DTA) are the transition and reaction temperatures, and it is employed in phase diagrams and thermal stability [1].

DTA is widely employed to determine the sintering window in powder metallurgy, along with thermo-gravimetric analysis (TGA) to know whether the atmosphere used is protective enough [2]. It is also used to determine kinetics of the reactions, for instance kinetics of crystallization of amorphous Fe–B alloys [3]. By means of DTA, reaction mechanisms of the aluminium borates with aluminium nitride [4] and oxidation mechanisms of ceramic materials (as AlN–TiB₂–TiSi₂) [5] have also been studied. In addition, DTA, along with other techniques, is used to characterize intermetallics [6].

This paper is part of a wide research dealing with the manufacture of high boron materials in the nuclear industry, with the aim of obtaining gamma radiation shielding

materials. They can also be used for military applications, due to their importance in the development of solid fuels [7,8], although the presence of iron delays the combustion process [9]. Boron and B₄C [10] are employed to control the activity of highly radioactive nuclear waste in nuclear reactors [11], being materials with high stability under neutron irradiation [12]. However, all boron materials accumulate large radiation-induced damages, caused, for instance, by helium formation and swelling. In the nuclear industry, two different aluminium-based materials reinforced with B₄C are being used, but they present corrosion and homogeneity problems due to their forming method [13–15]. The use of powder metallurgy as the forming technique allows in obtaining materials with controlled porosity, that is able to evacuate helium bubbles and so they can absorb the deformation caused by swelling, and also reduces the heterogeneities found in cast Al–B materials that causes non-uniform neutron absorption. This paper deals with the thermal analysis carried out to understand the phenomena that take place in the Al–B–Fe system, to use this material in the indicated field of application.

2. Experimental procedure

In this work, 20% (by wt.) of Fe/B powder obtained by mechanical alloying (36 h) [16] was added to the aluminium matrix. Mixing was carried out in a low-energy rotating

*Corresponding author. Fax: +34 91 624 94 30.

E-mail address: juana.abenojar@uc3m.es (J. Abenojar).

mill, until homogeneity was achieved. The homogeneity of the mixture was checked by means of its observation through optical microscopy.

DTAs of powder mixture were carried out under $N_2/10H_2/0.1CH_4$ atmosphere. The equipment was Netzsch STA409, fully calibrated at temperatures up to $1400^\circ C$ with different metal patterns (Zn, Sb, Al, Cu, Ni) [17], reaching their melting point, in order to assure measured temperatures and to calculate the enthalpies associated with the observed reactions. Heating and cooling rates were always $5^\circ C/min$. Six different tests were carried out, stopping the heating step at different temperatures (700, 800, 900, 1000, 1200 and $1250^\circ C$). In order to quantify the quantity of metal that reacts with Fe/B during sintering, the difference between melting and solidification heat of the aluminium was evaluated. In order to compare these results, samples were compacted and sintered at different temperatures under the same atmosphere, and afterwards a microstructural study was performed. Further, ten SEM micrographs (to represent the whole material) of each

material were taken on transverse cuts of obtained specimens. These micrographs were studied by image analysis (Image Pro Plus) to quantify the proportions, sizes and forms (roundness) of the present phases. The identification of phases was done through semiquantitative EDS coupled to SEM.

3. Results

In the microstructural analysis, formation of different phases from the initial ones, as well as the effect of temperature in the formation and growth of these phases is observed. In the micrographs of Fig. 1 (all of them taken at $100\times$), the formation and growth of phases can be observed.

Fe/B powder is an amorphous and non-stoichiometric compound obtained under non-equilibrium conditions, therefore it is expected that it separate in other more stable compounds, following the reaction below:

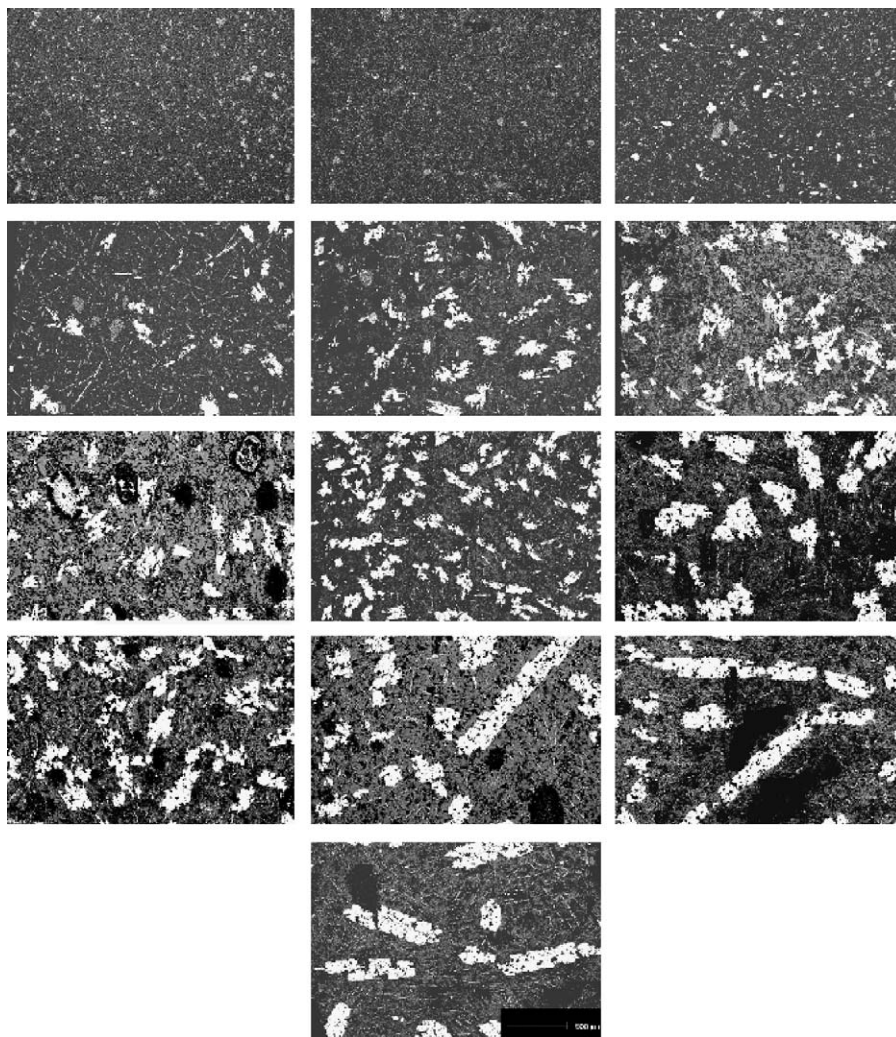


Fig. 1. Sequence of Al+20% Fe/B microstructures, sintered in $N_2/10H_2/0.1CH_4$ at different temperatures. All micrographs have the same magnification ($\times 100$).

White phases in these micrographs (Fig. 1) correspond to an intermetallic of the Al–Fe system (with composition of 50 wt% approximately). This intermetallic appears at 700 °C. At low sintering temperatures, a light grey phase corresponds to the original particles of Fe/B. These Fe/B particles can be clearly observed up to 900 °C. At 950 °C, some of these particles still remain but its location is more difficult, and above 1000 °C original Fe/B particles do not remain. In these micrographs, it can also be observed that intermetallic particles grow with the temperature. This growth is more marked when the temperature increases from 950 to 1000 °C. This fact agrees with the hypothesis that original Fe/B particles do not remain and all energy is spent in the Al–Fe particle growth. In addition, above 1100 °C these particles become longer. Moreover, besides these particles of Al–Fe, small acicular structures of the same intermetallic (same composition) can also be observed from 750 to 1200 °C. Micrographs of the Fig. 1 also show formed Al–B compounds (black phases).

Therefore, part of the aluminium is used in the formation of the Al–Fe compound and it should be observed that the differences between the melting and solidification peak areas in the DTA, since the amount of melted aluminium is not the same that afterwards solidifies. This fact was studied carrying out DTAs at different temperatures, from 700 to 1250 °C. As it can be observed in Fig. 2, this difference is larger at 1250 °C because all the aluminium melts (large endothermic peak), but since an important part of it reacts, aluminium that solidifies (exothermic peak) is less.

Fig. 3 shows the superposition of the melting and solidification peaks of pure aluminium (340 J/g), since there is not any transformation. There is a difference between the solidification and melting enthalpy, due to Fe/B presence, which grows with the temperature. Melting peaks of aluminium in the studied material (Al + 20% Fe/B) show similar values, since the melting reaction is unique. In addition, melting heat of the mixture is about 80% of the melting heat of aluminium, as expected since the mixture has 80 wt% of aluminium.

The difference between solidification and melting peaks is due to the reactions that take place. After reacting and during

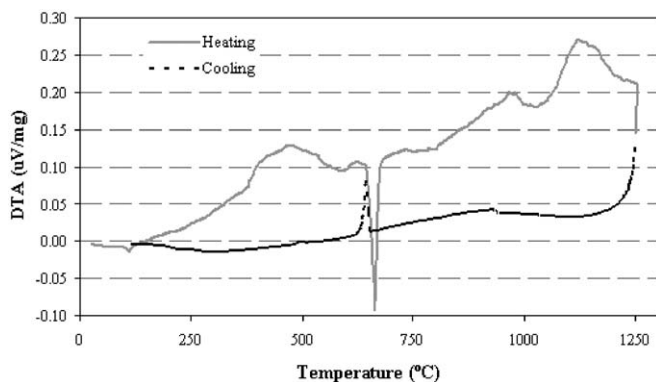


Fig. 2. Al + 20% Fe/B DTA performed up to 1250 °C in $N_2/10H_2/0.1CH_4$.

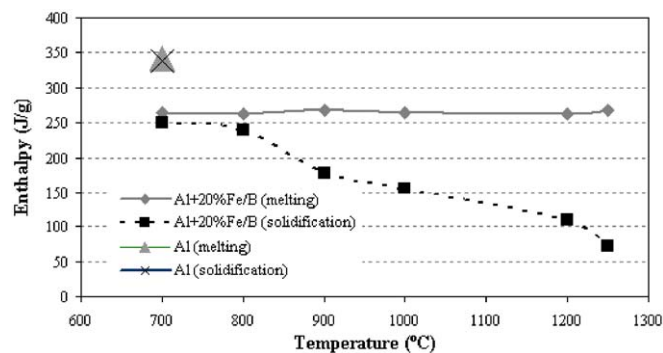


Fig. 3. Enthalpy of melting and solidification peaks in DTAs performed at different temperatures.

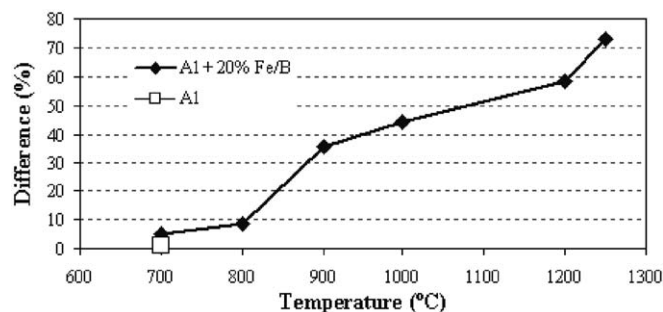


Fig. 4. Difference of enthalpy between melting and solidification peaks in Al + 20% Fe/B DTAs at different temperatures.

the cooling process, less aluminium remains and thus, enthalpy of the solidification peak is lower as DTA temperature increases. Fig. 4 shows these differences in percentage, reaching more than 70% for 1250 °C, the difference between 800 and 900 °C being remarkable, since at this temperature almost 40% of the aluminium has already reacted. Exactly at these temperatures there is a marked growth of the Al–Fe intermetallic grains, as Fig. 1 shows.

In order to study this phenomenon, microstructures (Fig. 1) were evaluated by image analysis techniques. Differences found between enthalpy of the peaks (Fig. 4) should agree with the Al–Fe percentage evaluated by means of image analysis. For this purpose, six micrographs of each material (all of the them at the same magnification, 100 ×) were employed. Some of these differences can be justified through this phase formation (Fig. 5), but at 1100 °C the difference between the aluminium melting and solidification peaks is about 50%, as can be observed in Fig. 4, and this difference is 21% according to image analysis (Fig. 5). The difference is due to the formation of Al–B compounds. These compounds cannot be quantified through image analysis, although these compounds are present, as can be observed in the microstructural analysis. Nevertheless, at 800 °C the percentages of Al–Fe phase measured by both techniques are coincident, changing this behaviour above 850 °C. This shows that above this temperature the formation of aluminium borides starts, and it increases with the temperature.

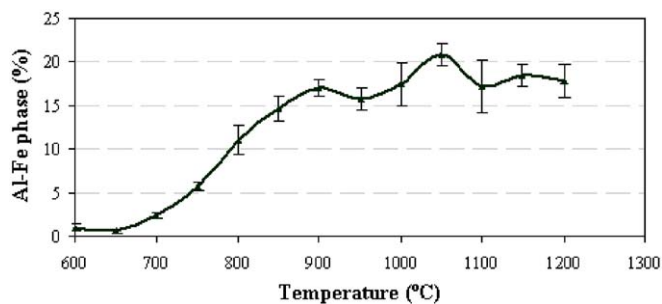


Fig. 5. Al-Fe phase average percentage observed by image analysis as a function of the sintering temperature.

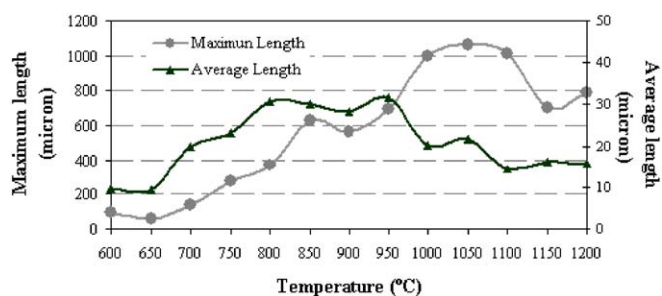


Fig. 6. Al-Fe phase grain length as a function of the sintering temperature.

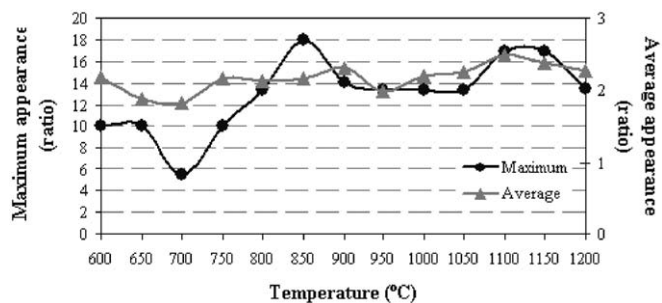


Fig. 7. Al-Fe phase appearance as a function of the sintering temperature.

Al-Fe grain size is studied by means of image analysis, by measuring its length (Fig. 6) and appearance (Fig. 7). The later parameter was measured through roundness, as the ratio:

$$\text{Perimeter}^2 / (4\pi \text{ area}).$$

In both the figures, the increase of grain size and less roundness with the temperature can be observed. The largest grain size is found at 1050 °C (Fig. 6), but the appearance with less roundness is found at 850 °C and maximum can be observed between 1100 and 1150 °C (Fig. 7). All these values agree with the micrographs shown in Fig. 1.

In summary, image analysis of the specimens shows that intermetallic formation rises up to 900 °C approximately,

barely changing above this temperature, although the size and shape changes take place.

4. Conclusions

Differential thermal analysis enables to evaluate the amount of intermetallic produced during the reaction between Al and Fe/B at different temperatures. These results have been verified by means of image analysis, finding a good agreement between both methods.

Intermetallic formation enables sintering of these alloys at higher temperatures than the base material melting temperature. Intermetallic grains present different sizes and shapes depending on the sintering temperature. In an initial stage, Al-Fe formation is promoted; when all the Fe/B within the material has already reacted, growth is enhanced. This change of behaviour occurs at about 900 °C.

Al-B compounds do not show the same behaviour; they show up at working temperatures but do not increase with temperature.

References

- [1] R.F. Speyer, Thermal Analysis of Materials, Marcel Dekker, New York, 1994.
- [2] J. Abenojar, F. Velasco, M.A. Martínez, J. Mater. Proc. Tech. 143 (2003) 28–33.
- [3] M. Matsuura, Solid State Commun. 30 (1979) 231–233.
- [4] G.J. Zhang, J.F. Yang, M. Ando, T. Ohji, S. Kanzaki, Acta Mater. 52 (2004) 1823–1835.
- [5] V.A. Lavreko, J. Desmaison, A.D. Pansyuk, M. Desmaison-Brurt, J. Eur. Ceram. Soc. 23 (2003) 357–369.
- [6] J.S.C. Jang, L.J. Chang, Intermetallics 10 (2002) 967–977.
- [7] W. Eckl, N. Eisenreich, W. Liehman, K. Menke, T. Rohe, V. Weiser, in: Combustion Phenomena of Boron Containing Propellants; Challenges in Propellants and Combustion—100 years after Nobel, Begell House Inc., New York, 1997, pp. 896–905.
- [8] J.M. Mota, J. Abenojar, M.A. Martínez, F. Velasco, A.J. Criado, J. Solid State Chem. 177 (2004) 619–627.
- [9] J. Abenojar, J.M. Mota, F. Velasco, E. Roth, V. Weiser, in: Energetic Materials; Reactions of Propellants, Explosives and Pyrotechnics (34th International Annual Conference of ICT), Fraunhofer Insitute für Chemische Technologie, Pfintzal, 2003, pp. 163/1–163/10.
- [10] W.K. Barney, G.A. Shemel, W.E. Seymour, Nucl. Sci. Eng. 1 (1958) 439–448.
- [11] H.C. Cowen, Nucl. Eng. 1 (1959) 11–17.
- [12] D. Simeone, C. Mallet, P. Dubuisson, G. Baldinozzi, C. Gervais, J. Maquet, J. Nucl. Mater. 277 (2000) 1–10.
- [13] C.J. Beidler, W.E. Hauth III, A. Goel, J. Test. Eval. 20 (1992) 67–70.
- [14] T.G. Haynes, K. Anderson, L.E. Oschmann, United States Patent 5965829, 12/10/1999.
- [15] Qualification of METAMIC for Spren-fuel storage application. EPRI, Palo Alto, CA: 2001.1003137. Reynolds Metals Co.
- [16] J. Abenojar, F. Velasco, J.M. Mota, M.A. Martínez, J. Solid State Chem. 177 (2004) 382–388.
- [17] H.G. Wiedemann, A. van Tets, Thermochim. Acta 1 (1970) 159–172.